Low Frequency Surf Zone Response to Wave Groups

Merrick C. Haller [1], Uday Putrevu [2], Joan Oltman-Shay [2], and Robert A. Dalrymple [1]

Abstract

The nearshore potential vorticity balance of Bowen and Holman (1989) is expanded to include the forcing from wave group-induced radiation stresses. Model results suggest that the forcing from radiation stresses can drive oscillations in the longshore current that have a spatial structure similar to linear shear instabilities of the longshore current. In addition, the forced response is nearly resonant when the forcing has scales (k, σ) similar to the linearly most unstable mode. Thus, we suggest that the wave groups may provide an initial perturbation necessary for the generation of shear instabilities of longshore currents and enough forcing to overcome frictional damping.

Analysis of data from the SUPERDUCK (1986) field experiment reveals that wave groups were present on days when strong low frequency surf zone motion (shear waves) existed. In addition, some of these groups are shown to have periods and longshore spatial structures comparable to the observed shear wave motions suggesting that incident wave groups are present on this open coast with the required spatial and temporal structure to initiate the low frequency oscillations in the longshore current.

1 Introduction

Shear waves are low-frequency (10^{-3} to $10^{-2} Hz$) vortical motions of surf zone currents. The kinematics of these waves are closely linked to the mean longshore current (Oltman-Shay et al., 1989). Bowen and Holman (1989) suggested that shear waves are generated due to a shear instability of the mean longshore current. Subsequent

[1] Center for Applied Coastal Research, Ocean Engineering Lab, University of Delaware, Newark, DE 19716, USA. Correspondence e-mail: merrick@coastal.udel.edu

[2] NorthWest Research Associates, Inc., P.O. Box 3027, Bellevue, WA 98009, USA.

work (see Shrira et al., 1997 for a complete set of references) has shown that the shear instability model is capable of explaining many of the observed characteristics. However, the instability theory fails to predict the following two features – both related to the effects of bottom friction. First, the instability theory predicts a low-frequency cutoff below which no shear waves are generated (Dodd, 1994; Shrira et al., 1997). Second, instability theory predicts that shear waves should be damped by friction on planar beaches. Both of these predictions are at odds with observations at Duck, NC and Santa Barbara (Leadbetter), CA beaches (Dodd et al., 1992).

Recently, the work of Shrira et al. (1997) showed that both shortcomings of the instability theory could potentially be explained by an explosive instability mechanism. In particular, they showed that shear waves that would otherwise be damped out by friction could grow due to resonant triad interactions provided their initial amplitudes exceed a critical value. However, how such initial (small amplitude) shear waves are generated remains unexplained. In this paper, we show that the direct forcing from wave groups could provide the initial amplitudes required by the resonant interaction model of Shrira et al. (1997). This mechanism follows earlier work by Hamilton and Dalrymple (1994).

The outline of this paper is as follows. Section 2 discusses the theoretical formulation. An example calculation in section 3 shows that direct forcing from wave groups leads to a larger response at shear wave scales, which may provide the initial amplitudes required by the resonant interaction model. In section 4 we analyze data from the SUPERDUCK experiment and find that there is evidence that the forcing required to set up these initial oscillations existed. Data from the experiment at Leadbetter Beach (a planar beach) could not be used in the wave group analysis because the offshore wave array was too short to resolve wave group scales. The final section is devoted to a few concluding remarks.

2 Theoretical formulation

The depth-integrated, short-wave-averaged equations of horizontal momentum read

$$\frac{\partial u}{\partial t} + u\frac{\partial u}{\partial x} + v\frac{\partial u}{\partial y} = -g\frac{\partial \eta}{\partial x} + \tau_x - \frac{\tau^b_{xz}}{\rho h}, \tag{1}$$

$$\frac{\partial v}{\partial t} + u\frac{\partial v}{\partial x} + v\frac{\partial v}{\partial y} = -g\frac{\partial \eta}{\partial y} + \tau_y - \frac{\tau^b_{yz}}{\rho h}, \tag{2}$$

where u and v are depth-averaged horizontal velocities in the cross-shore (x) and longshore (y) directions, respectively; η is the free surface displacement; g is the acceleration due to gravity; $\tau^b_{\alpha z}$ ($\alpha = x, y$) are the bottom shear stresses; and h is the total depth (it includes wave-induced set-down and set-up). Finally, τ_x and τ_y represent the forcing due to the radiation stresses.

We consider the case of a long straight coast. We separate all quantities into steady and time varying parts and assume that steady terms are independent of the longshore coordinate, e.g.,

$$\eta(x,y,t) = \eta_0(x) + \eta_1(x,y,t), \tag{3}$$

where η_1 represents the small ($|\eta_1| \ll |\eta_0|$) modulation effect of the wave groups. All other quantities are defined in an analogous fashion. We assume that the steady current has only a longshore component. That is, we assume

$$u = u_1(x,y,t) \tag{4}$$

$$v = V(x) + v_1(x,y,t). \tag{5}$$

Following Dodd et al. (1992), we parameterize the bottom friction using a linear law. In particular, we assume that $\tau^b_{xz} = \rho\mu u$, and $\tau^b_{yz} = \rho\mu v$, where $\mu = \frac{2}{\pi}c_f U_o$ is the friction coefficient, and U_o is the amplitude of the orbital velocity of the incident short waves and is assumed constant.

These definitions for velocity and bottom shear stress are now substituted into equations (1) and (2). The resulting equations are separated into steady and unsteady parts. We find that the steady problem reduces to the familiar cross-shore momentum balance determining wave set-up and set-down, and the longshore momentum balance governing the generation of the mean longshore current. The unsteady problem is of particular interest here since it governs the dynamics of the low frequency motion in the nearshore.

Following Bowen and Holman (1989), we make the rigid lid assumption, thus, the nondivergence of the continuity equation allows us to introduce a transport stream function, Ψ, such that $\Psi_y = -u_1 h$ and $\Psi_x = v_1 h$ (subscripts (x, y) denote partial differentiation). This leads to the following equation for the stream function:

$$\left(\frac{\partial}{\partial t} + V\frac{\partial}{\partial y} + \frac{\mu}{h}\right)\left(\frac{\Psi_x h_x}{h^2} - \frac{\Psi_{yy}}{h} - \frac{\Psi_{xx}}{h}\right) + \Psi_y\left(\frac{V_x}{h}\right)_x + \frac{\mu h_x \Psi_x}{h^3} = \frac{\partial \tau_{x,1}}{\partial y} - \frac{\partial \tau_{y,1}}{\partial x}, \tag{6}$$

where subscripts denote partial differentiation (except for the definition of $\tau_{\alpha,1}$, $\alpha = x, y$). For simplicity, we concentrate on periodic solutions. Hence, we assume that the stream function may be expressed as

$$\Psi = \Re e\left\{\psi(x)\, e^{i(ky-\sigma t)}\right\}, \tag{7}$$

where $\sigma = 2\pi/T$ (T = wave period) represents the wave frequency and $k = 2\pi/L$ (L = longshore wavelength) is the wavenumber. The amplitude of the stream function, $\psi(x)$, is in general complex. In addition, the forcing due to radiation stresses will also be assumed proportional to $e^{i(ky-\sigma t)}$, and expressed as

$$\frac{\partial \tau_{x,1}}{\partial y} - \frac{\partial \tau_{y,1}}{\partial x} = \Re e \left\{ F(x,k)\, e^{i(ky-\sigma t)} \right\} . \tag{8}$$

Note that the homogenous version of (6) ($F = 0$) is an eigenvalue problem. Nontrivial solutions for ψ exist only for certain values of the eigenvalues, σ. These frequencies represent the natural frequencies of the system. If the system is forced at (or near) these frequencies, then there is the potential for a large response.

In general, the natural frequencies of (6) are all complex, whereas the forcing frequency has to be real. Therefore, the possibility of exact resonance is somewhat limited for this system. However, there is still a potential for a large response if the frequency mismatch is small.

3 An example calculation

In this section we present an example calculation that illustrates the nature of the forced response. First, we need to specify the longshore current, the wavenumber and frequency of the forcing, and the friction factor. Wherever possible, we choose these parameters such that they are representative of those measured at Santa Barbara's Leadbetter beach. We make this choice because, as mentioned in the introduction, Dodd et al. (1992) found that the shear instability theory predicts that shear waves should be damped out by friction on this planar beach.

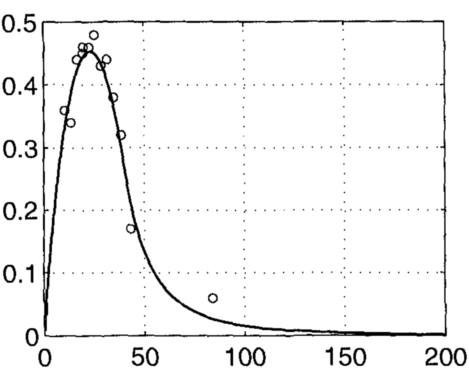

Figure 1: Cross-shore variation of the modeled longshore current (solid line) using the model of Longuet-Higgins (1970), circles represent measured data from Leadbetter Beach, Santa Barbara, February 4, 1980. Note: $x = 0$ is the position of the mean shoreline.

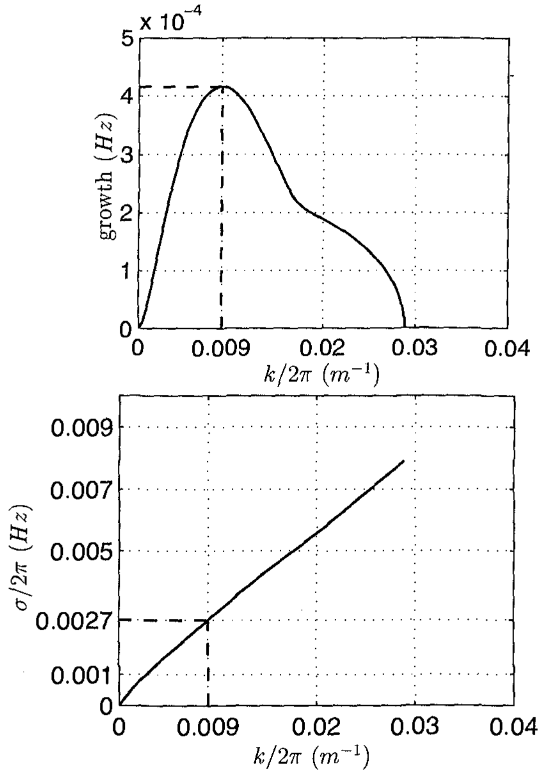

Figure 2: a) Linear growth rate and the b) dispersion relation for the most unstable modes of the homogeneous system for the longshore current profile shown in Figure 1.

The longshore current profile used in our calculations (along with the measured current values) is shown in Figure 1. To first get an estimate of the natural frequencies of the system, we solve the inviscid, homogeneous version of (6) (i.e. $\mu = 0$, $F = 0$). The results are shown in Figure 2. Figure 2a shows the growth rates of the most unstable mode for each wavenumber and Figure 2b shows the real part of the frequency. Dodd et al. (1992) obtained a similar dispersion curve and stated that it compares reasonably well with observations, however, they also found that the inclusion of realistic bottom friction will damp out the instability. Thus, the observations are unlikely to have resulted due to an instability of the longshore current profile. Here we investigate whether radiation stress forcing could have provided the small amplitude shear waves required of the explosive instability mechanism

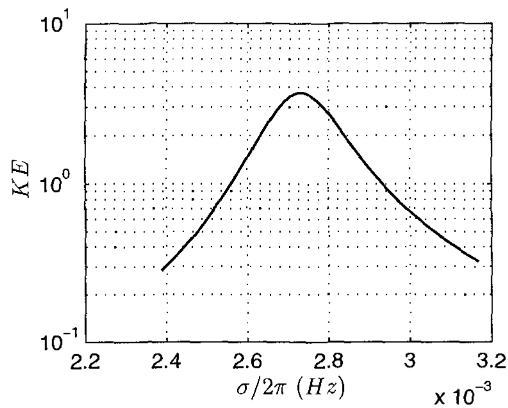

Figure 3: The variation of kinetic energy (KE) as a function of the forcing frequency for a forcing spatial scale of $k = 0.0566\, rad/m$. Shown is the forced system response (equation 6, $F = 0.05 h_x e^{-(x-x_b)^2}$) for the frictional dissipation coefficient: $\mu = 0.00372$.

Shira et al., 1997. To do that we have to first specify the forcing function. In our example calculation (6), we use

$$F = -.0025\, i\, g\, k\, h_x\, e^{-(x-x_b)^2}, \tag{9}$$

where x_b is the distance from the mean shoreline to the breaker location. We obtained this form of the radiation stress forcing term based on the stationary forcing used by Bowen (1969, see Eq. 32). In its present form, we have assumed the forcing to be longshore propagating and have limited the forcing amplitude to a region very close to the zone of initial breaking. This was done in order to include in a simple way the tendency for the breaker line to oscillate in the cross-shore direction with the modulations of the incident waves which destroys most wave grouping shoreward of the initial breaking region. However, the results are not sensitive to the form of the forcing decay away from the breaker line.

As a measure of the forced response, we use the total kinetic energy averaged over a wavelength and period and integrated over x:

$$\overline{KE} = \int_0^\infty \frac{1}{TL} \int_0^T \int_0^L \frac{(u_1^2 + v_1^2)h}{2} dy\, dt\, dx. \tag{10}$$

The variation of shear wave kinetic energy, as a function of forcing frequency, is shown in Figure 3 for a forcing spatial scale of $k = 0.0566\, rad/m$. This k value has the largest growth rate in the unforced, homogeneous system (Figure 2a) and the value of $\mu = 0.0269\, m/s$ is suggested by the model-data comparisons of Dodd

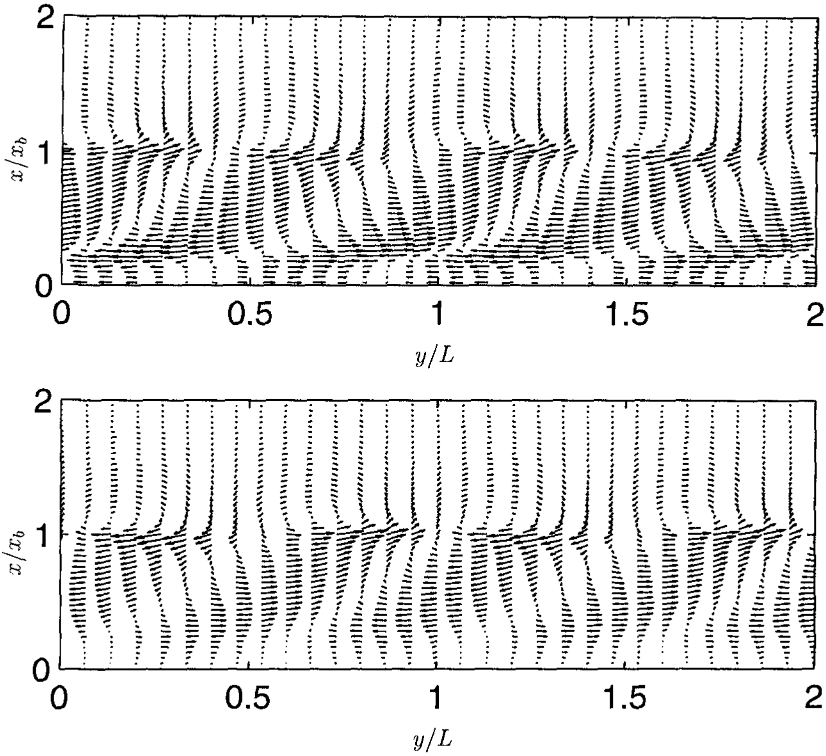

Figure 4: a) Velocity distribution from solution of homogeneous system, $k = 0.0566\, rad \cdot m^{-1}$. b) Velocity distribution from solution of forced system including dissipation, $k = 0.0566\, rad \cdot m^{-1}$, $\mu = 0.00372$.

et al. 1992. It is important to note that, though not shown here, the μ value does not alter the frequency of the maximum kinetic energy ($0.0027\, Hz$); the peak frequency consistently falls near the resonant frequency of the unforced system ($\sigma/2\pi = 0.0027\, Hz$ in Figure 2b).

A comparison of the forced and free shear wave velocity fields is presented in Figure 4 a and b. Figure 4a shows the velocity field of the free, undamped, shear instability ($\mu = 0, F = 0$). The magnitude and pattern of this field is remarkably similar to the forced, damped shear wave field (Figure 4b, $\mu = 0.00372$, F as defined in eq. 9). Note that the longshore phase difference between the two figures is arbitrary.

Figures 3 and 4 suggest an alternative shear wave generation mechanism for a beach such as Leadbetter where shear waves cannot be generated from an instability of the longshore current (assuming realistic frictional damping). These figures show that given forcing with spatial and temporal scales near those of the shear waves, the system can preferentially excite frequency-wavenumber scales that satisfy the free system and generate wave patterns with similar magnitude and form to the free, undamped shear waves. It is then plausible that these forced motions could resonantly grow via the explosive instability mechanism suggested by Shrira et al. (1997).

4 Field Data Analysis

The results from the calculations in Section 3 suggest that if wave group energy is present near the most unstable shear wave mode (from linear theory) in frequency-wavenumber space, the possibility of a near-resonant surf zone response to this forcing exists and an explosive instability generation can occur. In the following, field data from the SUPERDUCK experiment are analyzed for the presence of radiation stress forcing at the scales of shear waves.

The SUPERDUCK experiment was conducted by the U.S. Army Corps of Engineers in October of 1986 at Duck, North Carolina. The beach at this site trends NW-SE and is centrally located within a 100-km barrier spit (Crowson et al., 1988). The beach slope is typically 1:20 in the surf zone and decreases to 1:200 offshore. In addition, the bathymetry is characterized by a three-dimensional bar system which often becomes linear during storms (Lippmann, 1989).

Surf zone velocity records were obtained from a longshore array of ten Marsh-McBirney bidirectional electromagnetic current meters located approximately 55 m offshore from the mean shoreline in the trough of the bar (Oltman-Shay et al., 1989). The array had a minimum sensor separation of 10 m and total longshore extent of 510 m.

The incident wave climate was obtained by a linear array of 10 bottom-mounted pressure sensors located approximately 800 m offshore in 8 m water depth and spanning 255 m in the longshore direction. The array elements had a minimum sensor separation of 5 m. The wave fields measured during the experiment were highly variable but often consisted of longer period swell from the south along with shorter period wind-generated waves from the north and the surf zone usually extended approximately 100 m from the shoreline. Data for all sensors were sampled at 2 Hz during 4-hour measuring periods centered about high and low tides and the 4-hour tidal range was $\sim$ 20 cm with a shoreline excursion of 2 m.

The work of Oltman-Shay et al. (1989) showed that the vortical motions, due to shear instabilities of the longshore current (or shear waves), reside in the lower end of the infragravity band ($0.001 < f < 0.01$ Hz) with longshore wavelengths $100 < L < 1000$ m. Typical two-dimensional (f, k) spectra of measured surf zone velocities (u,v) from the SUPERDUCK data set contain a ridge of energy spanning this range of frequencies and wavelengths.

Offshore Wave Groupiness

To look for radiation stress forcing with similar scales to shear waves, we examine the incident wave envelopes associated with wave groups using the pressure records from the offshore (8 m depth) array. Each of the pressure records were divided into sections 2048 s in length, demeaned and then detrended (using a least squares quadratic fit). The pressure records were converted to records of water surface elevation using the pressure response factor according to linear theory. The wave records were then bandpass filtered (0.06 – 0.30 Hz) to remove low (infragravity) frequency and high (wave harmonics, turbulence) frequency energy outside of the wind wave band. Time series of wave envelopes were computed from the filtered wave records using the Hilbert transform method (Melville, 1983). The specific data runs used in the present analysis represent a subset of the entire SUPERDUCK data set. Data selection was based on whether energetic shear wave motions were present in the nearshore current records during the data run and by data quality and availability considerations. The incident wave conditions during the data runs used herein are considered typical for the field site. If a groupiness factor for each record is defined by $\sqrt{2} \cdot \sigma_A/\overline{A}$, where σ_A is the standard deviation of the wave envelope, $\overline{A}$ is the mean, and GF varies from $0 \rightarrow O(1)$ then the average GF for these records is ~ 0.75; suggesting significant wave grouping was present offshore of the surf zone on the days analyzed herein. In addition, previous work using data from this field site has indicated that wave grouping can persist into the surf zone (List, 1991; Haller and Dalrymple, 1995).

Offshore Wave Groups and Surf Zone Shear Waves

Phase and coherence between the wave group time series of the offshore pressure sensors were calculated and plotted, as a function of sensor alongshore separation, to estimate the longshore scale and propagation direction of the incident wave groups. The offshore wave group phase and coherence plots were then compared with the (surf zone) shear wave phase and coherence plots computed from the longshore current records. All cross-spectra were computed using the standard Fast Fourier Transform method after first dividing each time series into 13 ensembles 2048 s in length with 50% overlap and tapering with a Hamming window. The number of spectral components was then reduced by half using a 2-point average resulting in a resolution of $\Delta f = .001$ Hz and 44 degrees of freedom (d.o.f.).

Using the longshore current records, the range of frequencies which contained spatially coherent shear waves was determined for each data run (usually 0.001 – 0.006 Hz). Typically, the shear waves demonstrated strong coherence for longshore distances of $\sim$ 200 m. Oltman-Shay et al. (1989) showed that cross-shore current records also indicated coherent shear waves of similar scale. However, offshore wave group spatial coherence was found to typically be less than 100 m. The tendency for wave groups to have low spatial coherence is not unexpected since wave grouping is likely a random process and is therefore broad banded in wavenumber at a given frequency. This is in contrast to shear waves, which are the result of

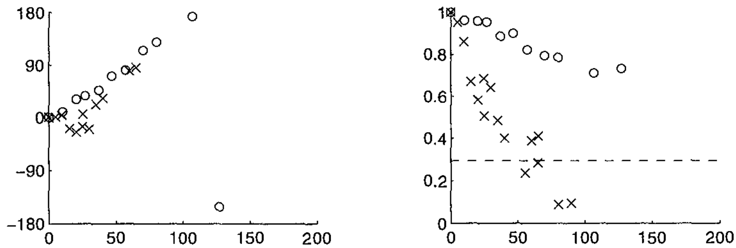

Figure 5: Comparison of (*a*) relative phase vs. lag, (*b*) coherence vs. lag for shear waves (**o**) and offshore wave groups (**x**) at frequency 0.003 Hz. Dashed line represents 85% confidence interval, 44 d.o.f.. Data is from October 15 at 0945 EST sensors LA 1-6, LX 1-5.

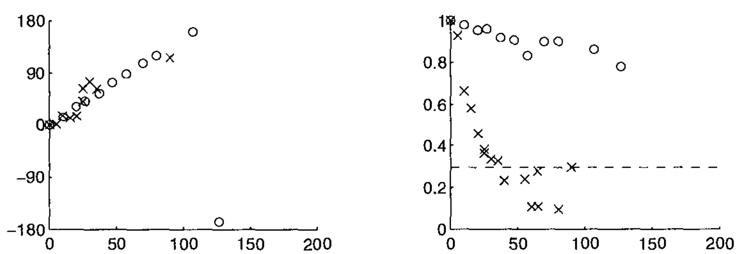

Figure 6: Comparison of (*a*) relative phase vs. lag, (*b*) coherence vs. lag for shear waves (**o**) and offshore wave groups (**x**) at frequency 0.003 Hz. Dashed line represents 85% confidence interval, 44 d.o.f.. Data is from October 16 at 1020 EST sensors LA 1-6, LX 1-5.

a resonant process and tend to be narrow banded in wavenumber. In addition, wave group spectra tend to exhibit more statistical uncertainty then the original wave/current records and very long wave records are needed in order to obtain truly stationary estimates of wave grouping (Nelson et al., 1988). To limit the processing of incoherent data, the offshore array was limited to six closely spaced sensors with a maximum lag of 90 m. The nearshore array was similarly limited to five sensors with a maximum lag of 130 m.

Using the wave group cross-spectra, the range of existing shear wave frequencies were searched for the presence of spatially coherent wave groups. Relatively few cases were found in which the offshore wave groups were clearly shown to have scales similar to shear waves. In many cases the wave groups did not exhibit significant coherence. In addition, there were cases where coherent wave groups existed but with scales different from shear waves and those will not be discussed here. The cases which best demonstrate that wave groups can exist offshore at similar spatial scales as shear waves are shown in Figures 5-6.

For comparison, the relative phase and coherence vs. longshore lag of the shear waves is plotted together with those of the offshore wave groups. The slope (+/-) of phase vs. lag indicates the direction of propagation (upcoast/downcoast) for the given motion and the figures show that the offshore wave groups at these frequencies were propagating in the same direction as the shear waves. The comparisons of coherence indicate that wave groups lose coherence at much shorter distances than shear waves ($\sim$ 50 m). The 85% confidence interval is also shown for reference (dashed line). The relative phase for lags which did not demonstrate coherence above the 85% confidence level are not plotted.

Surf Zone Wave Groups and Shear Waves

The computations in Section 3 assumed that incident wave heights had a longshore progressive 2-D structure near the breaker line that swiftly decayed shoreward due to wave breaking. It is expected that any wave grouping present at the offshore array would persist and possibly increase in amplitude towards the breaker line due to shoaling. However, since the offshore array was about eight surf zone widths (x_b) from the shoreline, the cross-shore current records measured at the nearshore array (located $\sim x_b/2$) were also examined for any evidence of wave grouping persisting shoreward of the breaker line. To do this, it was necessary to assume that, in the range of incident wave frequencies ($0.06 < f < 0.3$ Hz), the auto-spectra of the u velocities have the same shape as sea surface elevation spectra at the same location, since there were no pressure sensors in the nearshore (longshore) array. Figure 7 indicates this assumption is reasonable. The choice of cross-shore velocities for the wave group analysis was made because the u auto-spectra were more energetic at incident wave frequencies due to the near normal incidence of the waves at this nearshore location. The u velocity records were converted to surf zone wave (current) envelopes in the same manner as the offshore wave records (neglecting the pressure to water surface conversion).

A result from the phase and coherence analysis of the surf zone wave envelopes is shown in Figure 8. The linear phase progression in the longshore direction demonstrates that a certain amount of wave grouping was present in the surf zone during the data run taken the morning of October 18. It should be noted that the bandpass filtering operation was tested with different windows (Hamming, Hanning) to rule out the possibility of leakage of the energetic shear wave motions into the incident wave band during filtering. The offshore wave envelopes did not show strong spatial coherence at this frequency suggesting that wave grouping was locally induced during this data run.

The results of the cross-spectral analysis for this subset of SUPERDUCK data

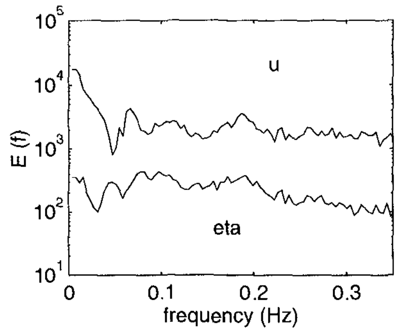

Figure 7: Comparison of auto-spectra of cross-shore velocity and water surface elevation from nearly co-located surf zone sensors. Data is from October 18 at 1140 EST.

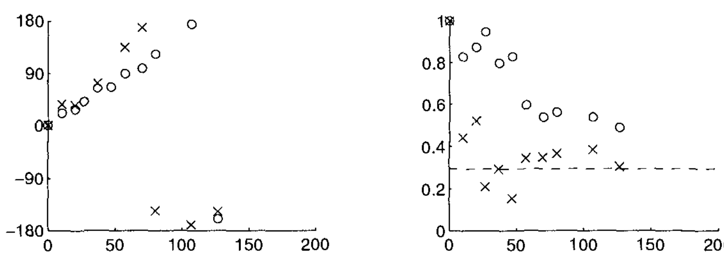

Figure 8: Comparison of (*a*) relative phase vs. lag, (*b*) coherence vs. lag for shear waves (**o**) and surf zone wave groups determined from cross-shore velocity records (**x**) at frequency 0.003 Hz. Dashed line represents 85% confidence interval, 44 d.o.f.. Data is from October 18 at 1140 EST sensors LX 1-5.

demonstrate that wave grouping at shear wave and other scales can exist in the field. The calculations presented in Section 3 indicate that the response to such forcing will occur primarily at shear wave scales and that the velocity field will closely resemble the velocity field under free shear waves. Thus, it is likely that direct forcing from wave groups might provide the initial perturbations required for shear wave growth.

5 Conclusions

The inclusion of a forcing term due to wave group induced radiation stresses in the nearshore potential vorticity balance of Bowen and Holman (1989) shows that incident wave groups can force a surf zone response similar to shear waves. If the forced response has similar scales (k, σ) to the linear most unstable mode, the response is nearly resonant.

Field data were examined for the presence of wave group forcing with scales similar to the observed shear waves. Analysis of phase and coherence shows that wave grouping of shear wave scales was sometimes present during the SUPERDUCK experiment. The results suggest that wave grouping can exist to perturb the nearshore velocity field at temporal and spatial scales of the shear instabilities.

In addition, it is interesting to view the results presented here in light of the recent work of Shira et al. (1997). Their work indicates that the range of unstable scales for shear waves excited by the explosive instability mechanism is much larger than that determined by the linear instability mechanism. This suggests that the presence of any of a wide range of coherent wave group spatial scales can force any of a wide range of initial instabilities to feed the explosive instability mechanism. Also, they show that the explosive instability occurs, even when all linear instabilities are damped by bottom friction, as long as the initial perturbations exceed a certain amplitude.

The wave group forcing mechanism presented here and the results of Shrira et al. (1997) provide a possible explanation for the observation of shear wave instabilities at Leadbetter Beach, CA. Dodd et al. (1992) found that linear instability theory did not predict instabilities for that beach unless the frictional damping was decreased by decreasing the friction coefficient, c_f, to unrealistic values. In light of the above, it can be hypothesized that the shear waves observed at Leadbetter Beach may have been generated via the explosive instability mechanism with wave groups providing the initial instabilites.

Acknowledgments

Funding for U. Putrevu and J. Oltman-Shay was provided by ONR Coastal Dynamics under contract number N00014-96-C-0075. Funding for M. Haller and R. Dalrymple was provided by the Army Research Office through University Research Initiative Grant DAAL 03-92-G-0116. The authors wish to thank Bob Hamilton for providing some of the software used in the data analysis and Bill Birkemeier, Peter Howd, Ed Thornton, and the staff at the Army Corps Field Research Facility (FRF) at Duck, NC, for their contributions to the field data acquisition and distribution (the 8 m array is still maintained as part of the FRF infrastructure).

References

Bowen, A. J., and R. A. Holman, Shear instabilities of the mean longshore current, 1. Theory, *J. Geophys. Res.,94*, 18023-18030, 1989.

Crowson, R. A., W. A. Birkemeier, H. M. Klein, and H. C. Miller, SUPERDUCK nearshore processes experiment: Summary of studies. CERC Field Research Facility, *Tech. Rep. CERC-88-12,* 81 pp., Coastal Eng. Res. Cent., Vicksburg, MS, 1988.

Dodd, N., J. Oltman-Shay, and E. B. Thornton, Shear instabilities in the longshore current: A comparison of observation and theory, *J. Phys. Oceanogr., 22,* 1, 62-82, 1992.

Haller, M. C., and R. A. Dalrymple, Looking for wave groups in the surf zone, Proceedings of Coastal Dynamics '95, 81-92, 1995.

Hamilton, R. P., and R. A. Dalrymple, Wave group forcing in low frequency surf zone motion, Center for Applied Coastal Research, *Res. Rpt. CACR-94-23,* 1994.

Lippmann, T., The stability and spatial variability of sand bar morphology, M.S. Thesis, 132 pp., Oreg. St. Univ., Corvallis, 1989.

List, J. H., Wave groupiness variations in the nearshore, *Coastal Eng.*, 15, 475-496, 1991.

Longuet-Higgins, M. S., Longshore currents generated by obliquely incident sea waves, 2, *J. Geophys. Res., 97,* (33), 6790-6801, 1970.

Melville, W. K. Wave modulation and breakdown, *J. Fluid Mech., 128,* 489-506, 1983.

Nelson, R. C., P. D. Treloar, and N. V. Lawson, The dependency of inshore long waves on the characteristics of offshore short waves, *Coast. Eng.*, 12, 213-231, 1988.

Oltman-Shay, J., P. A. Howd, and W. A. Birkemeier, Shear instabilities of the mean longshore current, 2. Field observations, *J. Geophys. Res., 94,* 18,031-18,042, 1989.

Shrira, V. I., V. V. Voronovich, and N. G. Kozhelupova, Explosive instability of vorticity waves, *J. Phys. Oceanogr., 27,* 542-554, 1997.